이학석사 학위논문

Implementation of Chemical Exchange-Dependent Saturation Transfer (CEST) and T1rho MRI at High Field

고자장 MRI 에서 CEST 와 T1rho 영상 구현

2014 년 08 월

서울대학교 대학원

의학과 협동과정 방사선응용생명과학전공

권 정 민

A thesis of the Degree of Master of Science

고자장 MRI 에서 CEST 와 T1rho 영상 구현

Implementation of Chemical Exchange-Dependent Saturation Transfer (CEST) and T1rho MRI at High Field

August 2014

The Department of Interdisciplinary Program in Radiation Applied Life Science,
Seoul National University
College of Medicine
Jeong Min Kwon

Implementation of Chemical Exchange-Dependent Saturation Transfer (CEST) and T1rho MRI at High Field

지도교수 김 현 진

이 논문을 이학석사 학위논문으로 제출함

2014년 04월

서울대학교 대학원

의학과 협동과정 방사선응용생명과학전공

권 정 민

권정민의 이학석사 학위논문을 인준함

2014년 06월

위 원 장 예 성 호 (인)

부 위 원 장 김 현 진 (인)

위 원 김 명 환 (인)

Implementation of Chemical Exchange-Dependent Saturation Transfer (CEST) and T1rho MRI at High Field

by
Jeong Min Kwon

A thesis submitted to the Department of Interdisciplinary Program in Radiation Applied Life Science in partial fulfillment of the requirements for the Degree of Master of Science at Seoul National University College of Medicine

June 2014

Approved by Thesis Committee:

Professor Sung-Joon Ye Chairman

Professor Hyeonjin Kim Vice chairman

Professor Myoung-Hoon Kim

ABSTRACT

Introduction: Rheumatoid arthritis (RA) is a public health problem that involves the disorder of articular cartilage. It has been reported that the loss of glycosaminoglycan (GAG) in cartilage is a signal of early RA onset. The macromolecules such as GAGs have much shorter TE and are not able to be identified using conventional MR Imaging techniques. In order to monitor GAGs concentration change in vivo, novel quantitative techniques such as T1rho mapping, gagCEST provide direct and indirect assessments of cartilage composition.

Methods: With the purpose of setting up the CEST sequences, phantom and *in-vivo* scans were performed. The MR signals under saturation pulse at different frequencies were fit into a smooth CEST "z-spectrum" and MTR asymmetry curve were calculated. A pulse sequence consisting of T1rho-prepped, FSE image acquisition. Multiple TSL(spin lock time; 10, 30, 50, 70, 100, 120 ms) were used to construct a T1rho relaxation map in the both phantom(a swine patella *ex-vivo*) and male wistar rat in the knee joint *in-vivo*.

Results: High MTR_{asym} (1.0 ppm) values reflect the GAGs contents in both swine patella phantom and cartilage in rat knee *in-vivo*. The quantitation of gagCEST MRI is based on the asymmetry in the CEST spectrum curve around 1.0 ppm and its reference frequency −1.0 ppm. The experiments attempt to explain how molecular properties of model tissue systems influence proton relaxation in the rotating frame and how they may be employed to generate useful contrast in images. The experiments will emphasize quantitative measurements of spin-lattice relaxation in the rotating frame.

Conclusions: CEST MRI and T1rho image as a molecular imaging technique was developed to detect the *in-vivo* MMs protons, which cannot be assessed by the traditional MRI methods. In this study, CEST and T1rho MRI was performed in swine patella phantoms and rats *in-vivo* to set up the MR imaging procedures and test its performance in finding macromolecules. Based on these preliminary results, we can get meaningful 9.4T gagCEST and T1rho cartilage images. And the ability of other MMs zones potential remains such as Alzheimer's disease, and tumors.

Keywords: mri, t1rho, gagcest, macromolecule, quantitative

Student number: 2012-23656

CONTENTS

LIST OF TABLES AND FIGURES

LIST OF ABBREVIATIONS

CEST : chemical exchange-dependent saturation transfer

ETL : echo train length

FOV : field of view

GAG : glycosaminoglycan

MM : macromolecule

MRI : magnetic resonance imaging

MTR : magnetization transfer ratio

MTR_{asym} : magnetization transfer ratio asymmetry

NSA : number of signals averaged

RF : radio frequency

ROI : region of interest

SNR : signal-to-noise ratio

SL : spin locking

T1rho: longitudinal relaxation time in rotating frame

T2 : transverse relaxation time

TE : echo time

TR : repetition time

TSL : spin locking time

INTRODUCTION

Compared to other medical imaging modalities such as computed tomography (CT) and X-ray, magnetic resonance imaging (MRI) has several advantages including no risk of ionizing radiation, excellent soft tissue contrast and the ability to produce images in any plane[1-3]. Furthermore, a variety of different image contrast provided by MRI allow for non-invasive extraction of functional information from living organs in addition to the conventional, anatomical information.

However, MRI-detectable signal is limited in that the lifetime of mobile protons (e.g., those in water molecules) after excitation, which is characterized in terms of transverse relaxation time or T2, ranges a few tens to a few hundred millisecond (ms), whereas that of less mobile protons such as those in MMs can be two to three orders of magnitude shorter. As such, non-invasive quantification of MMs are not possible with conventional MRI methods. Given that the amount of macromolecules (MMs)(e.g., peptides, proteins) are known to be altered in the progression of diseases such as tumors[4]

and osteoarthritis[5], therefore, developing an MRI method for MM quantification would further extend its applicability in basic research and medicine.

To address this issue, several approaches have been proposed such as chemical exchange-dependent saturation transfer (CEST) MRI [6, 7] and longitudinal relaxation time (T1) in rotating frame (T1rho) MRI [8, 9]. The CEST MRI takes advantage of the fact that there is continuous chemical exchange between the protons in free water and in MMs, that the resonance frequency of protons residing in a molecule is determined by their chemical environment (known as chemical shift[10]) thereby allowing spectral differentiation not only between water and MM but between different MMs as well, and that the amount of MMs is indirectly quantified via reduction of water signal after irradiation of a frequency-selective radio-frequency (RF) pulse on to the resonance frequency of MMs. In T1rho MRI, the quantification of MMs is achieved by irradiation of RF pulse that is designed to freeze or 'lock' spin evolution in the transverse plane. During such 'spin-locking', spins still lose their magnetization over time via T1 relaxation in rotating frame, and the T1 relaxation time in that rotating frame or

T1rho is assumed to be determined mainly by the amount of MMs whose range of frequencies of molecular motion (mainly molecular tumbling) is close to the Larmor frequency of the spin-locking RF pulse [11]. The potential clinical applicability of these MRI techniques has been reported previously at clinical field strength [12]. As these MRI techniques allow for quantitative analyses of MMs that may be associated with disease progression [12], they may facilitate development of a novel means of diagnosing and/or monitoring diseases via preclinical studies using high field animal MRI scanners.

However, implementation of these MRI techniques at high-field can be challenging due to the presence of severe B_0 and B_1 inhomogeneity.

To this end, the purpose of this research was to implement and optimize those CEST and T1rho MRI techniques at 9.4T animal MRI scanner, and validate their performance by acquiring preliminary *in vivo* data in laboratory animals.

METHODS AND MATERIALS

THEORY

CEST

Glycosaminoglycan (GAG) is known to be present in cartilage, and its concentrations is reported to be associated with cartilage degeneration [13]. GAG chemical exchange–dependent saturation transfer MRI (gagCEST MRI) is based on the chemical exchange between GAG hydroxyl protons and bulk water protons. In biological systems, hydrogen protons can roughly be categorized into three pools: a 'free pool' consisting of relatively mobile protons in free water molecules, a 'mobile pool' consisting of protons bound to large mobile MMs (like GAG hydroxyl protons), and a 'bound pool' consisting of protons in other macromolecules with restricted motion[5]. With conventional MRI, only the 'free pool' is detectable while the 'mobile pool' and the 'bound pool' are not visible due to their very short T2. The echo time (TE) of an MRI sequence is normally at the range of ms. Therefore, the magnetization of MMs in the transverse plane can already be completely dephased before the onset of signal acquisition.

In a CEST MRI pulse sequence, if a continuous RF pulse is applied at the resonance frequency of protons bound to MMs (such as GAG hydroxyl protons), it moves some protons in the lower energy level of the 'bound pool' to the higher energy level because of the input energy from the RF pulse. It then narrows down the difference of the numbers of protons between the two energy states and thus saturates the net magnetization of protons in MMs. Now, the chemical exchange between the protons of free water and GAG hydroxyl protons would result in relatively reduced MRI signal from those protons in free water, the extent of which depends on the amount of GAG hydroxyl protons. Therefore, the cartilage with higher GAG concentrations tends to generate a larger reduction of MRI signal from free water. Hence, a contrast between tissues with higher GAG concentrations and those with lower GAG concentrations is created. That is, by analyzing the decrease of the free water signal, the relative concentrations of GAG molecules in different types of tissue can be estimated by using CEST.

Until now many gagCEST studies have been performed *ex-vivo*, such as on removed bovine patella and GAG phantoms[14]. However, a few clinical observations have also been presented in cartilage [15].

CEST MRI Pulse Sequence

Compared to routine MRI pulse sequences, the major difference of CEST MRI pulse sequence is that a pre-saturation pulse with relatively narrow excitation bandwidth is applied before the common RF excitation and signal acquisition to saturate the magnetization of the 'bound pool' at its resonant frequency, which may differ for different types of MMs. For instance, the amide protons residing in proteins have the resonant frequency of 3.5 ppm relative to the resonance frequency of free water proton[16] ; hydroxyl protons in glycogens have the resonant frequency of 1.0 ppm [17]. The amplitude and duration of the saturation pulse are also important. Usually, the higher pulse power and the longer duration time result in a better saturation of the 'bound pool' which facilitates the CEST effect. But in practice, amplification of CEST effect is limited by safety

consideration (Specific Absorption Rate or SAR). A simplified CEST MRI pulse sequence diagram is shown below (in Fig. 1).

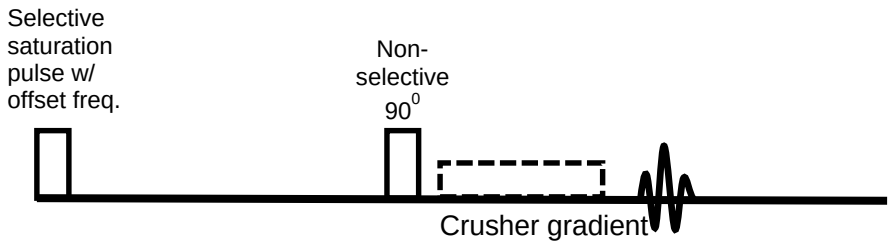

Figure 1 CEST pulse sequence diagram

Saturation Pre-Pulse Power Optimization

CEST system contains bulk water protons and labile protons within macromolecules. The RF saturation pulses on labile protons cause reduction of signal from free water protons, which exchange their unsaturated protons with the saturated labile protons. In practice, when RF power goes up, the bulk water MR signal may decrease as a result of off-resonance RF irradiation, independent of the saturation transfer phenomenon. This is known as the direct RF saturation effect. In fact, experiments have shown that CEST contrast initially increases with RF power, but plateaus and subsequently decreases at

higher RF power, suggesting RF saturation effects. As a result, for a given CEST system, there is an optimal RF power that maximizes the experimentally obtainable contrast.

Quantitative Analysis of CEST Contrast

To obtain CEST contrast, typically, an RF pulse is applied at an offset frequency (typically several ppm, $\delta\omega$) as referenced to the water peak (ω_0 = 0 ppm), and after saturated protons exchange with the water protons the reduced signal is then acquired. The off-resonance irradiation pulse may then be swept across a range of frequencies surrounding the water peak forming a "z-spectrum" of the resulting signal intensity at each obtained frequency step. If this spectrum is then normalized to a non-saturated image, the magnetization transfer ratio (MTR) is generated as shown in Eq. 1 where $S(\delta)$ is the signal intensity obtained with a resonance frequency offset δ, and $S(0)$ is the signal intensity obtained without the saturation RF pulse[18, 19]. Peaks in this z-spectrum can identify the resonance frequency offsets of specific exchanging species. However, the applied pulse may also alter the water signal because of direct saturation or non-specific

magnetization transfer [20] with other broad resonances, and therefore two images are acquired for CEST imaging in general. Each image is acquired at the opposite frequency offset (± ppm of MM resonance of interest). The difference in the normalized saturation contrast on opposite sides of the water peak is referred to as the magnetization transfer ratio asymmetry (MTR_{asym}) as estimated by using Eq. 2.

$$\mathrm{MTR} = 1 - \frac{S(\delta)}{S(0)} \qquad [1]$$

$$\mathrm{MTR}_{asym} = \frac{S(-\delta) - S(+\delta)}{S(0)} \qquad [2]$$

T1rho

Spin-lattice relaxation in the rotating frame, or T1rho, was described by Redfield in 1955 with experiments on aluminum and copper[21]. Decades have passed prior to T1rho research in biological applications such as in cartilage [22], Alzheimer's

disease and tumor[14, 23]. As a non-invasive imaging method, MRI provides excellent soft-tissue contrast with direct visualization of cartilage, joint fluid and endochondral bone. The contrast agent is rarely needed for the cartilage imaging.

Principle and Pulse Sequence of T1rho MRI

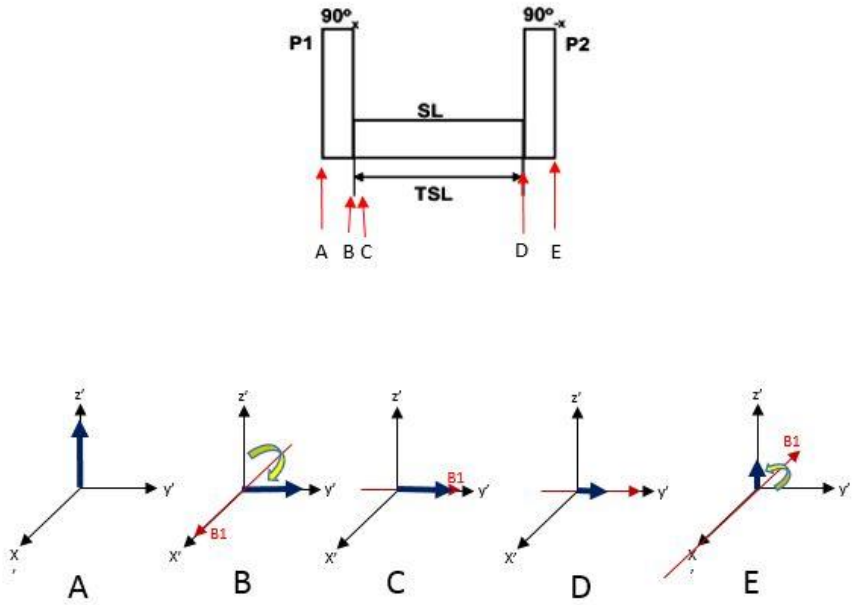

Figure 2 : A typical T1rho experiment. Magnetization precession and decay under spin-locking conditions. The M_0 vector is first nutated into the transverse plane by a 90-degree pulse. A long spin-lock pulse is applied, locking magnetization to the B_1 field. (SL: spin locking, TSL: spin locking time)

This pulse sequence, which is used in the present work, begins with a 90° hard pulse, which nutates the magnetization vector from its equilibrium position on to the transverse plane. The spin-locking pulse is then applied along the transverse magnetization for a specific duration (TSL), causing the magnetization component aligned with the spin-locking field to decay at a time constant of T1rho. Next, another RF pulse (-90°) is applied along with a crusher gradient for the removal of residual transverse magnetization. The remainder of the longitudinal magnetization is sampled at multiple TSLs and images are created using, for instance, a fast-spin echo sequence[24]. T1rho signal decay is similar to T2 decay, and therefore a simple curve-fitting is used to estimate T1rho by assuming a single exponential decay. In this study, T1rho is assumed to be determined mainly by the amount of MMs whose range of frequencies of molecular motion is close to the Larmor frequency of the spin-locking RF pulse [11]. Thus, T1rho measurements are thought to probe the slow molecular interactions that occur within the 0-100 kHz range. T1rho measurements were found to be increased in osteoarthritic subjects and with increasing grades of osteoarthritis[25]. Many

studies have found that there is at least some depth-wise variability in T1rho [26-28], with some studies further specifying that this variability corresponded to a variable proteoglycans (PG) and GAG content[23].

EXPERIMENTS

Phantom and Ex-vivo Sample Preparation

We first tested signal-to-noise-ratio (SNR) and image quality on a homogeneous 3% agarose phantom before the *in vivo* study. *Ex-vivo* experiments were also performed in swine patella filled in 3% agarose. All phantoms were kept at 37℃ by thermocouple connected to an animal physiologic monitoring system (SA Instruments, Stony Brook, NY, USA) during data acquisition.

Animal Preparation

The study included 16 six to ten week-old male wistar rats (Orient Bio, Seoul, Korea). The animal study was approved by the institutional animal care and use committee (IACUC) of the Seoul National University Hospital.

The rheumatoid arthritis was induced in animals. A mixture of incomplete Freund's adjuvant (2mg/ml in 0.05 mol/L acetic acid; Chondrex, USA) and the same amount of bovine type II collagen (Chondrex, USA) was slowly homogenized at 4℃. Then, the emulsion was injected into the tail vein of the rats. Rats were received the emulsion a total of 4 times every week (1^{st} and 2^{nd} week: 0.2ml, 3^{rd} and 4^{th} week: 0.2ml). Those rats in the treated group (n=5) were orally received Methotrexate (MTX; 1ml/100g) daily for two weeks. Those rats in the control group (n=6) received saline solution at the same amount and frequency.

Animal body temperature was monitored by thermocouple connected to an animal physiologic monitoring system (SA Instruments, Stony Brook, NY, USA) and was maintained at 37℃. The animal legs were placed in the center of the surface coil for cartilage imaging. During MRI experiments, animals were anaesthetized using isoflurane (2.5%) [29].

MRI data collection

All MRI data were collected on a 9.4T animal MR scanner (Agilent technologies, Palo Alto, California, USA) using a phased-array 4-channel surface coil (Agilent technologies, Palo Alto, California, USA).

For CEST MRI studies in phantom, the saturation pulse duration was 320 ms with a B1 field strength of 42 Hz. The CEST spectrum was acquired with 21 offset frequencies from 2 ppm to -2 ppm with a step size of 0.2 ppm. The sequence parameters were: TR/TE = 2000/8.3 ms, echo train length (ETL) = 8, number of signal averages (NSA) = 1, FOV = 51.2 x 51.2 mm^2, matrix size = 64 x 64, Bandwidth = 3 kHz.

For CEST MRI studies in animals, the CEST spectra were acquired with 13 offset frequencies from 2 ppm to -2 ppm with a step size of 0.25 ppm. The B1 field strength of the pre-saturation pulse was 50 Hz with a duration of 500 ms. MTR_{asym} was estimated at offset frequencies of ±1.0 ppm [5].

The sequence parameters were: FOV = 20.0 x 20.0 mm^2, matrix size = 256 x 256, number of slices = 1, slice thickness

= 1 mm, TR/TE = 3000/13.5 ms, ETL = 4, NSA = 1, bandwidth = 3.5 kHz, selective fat saturation.

For T1rho MRI in phantom, TSLs of 10, 20, 30, 40, 50, 70 and 100 ms were used. The sequence parameters were: FOV = 50 x 50 mm^2, matrix size = 256 x 256, number of slices = 1, slice thickness = 1.00 mm, TR/TE = 3500/8.68 ms, ETL = 8, NSA = 1, bandwidth = 3.5 kHz.

For T1rho MRI in animals, TSLs of 10, 30, 50, 70, 100 and 120 ms were used.

The sequence parameters were: FOV = 20 x 20 mm^2, matrix size = 256 x 256, number of slices = 1, slice thickness = 1.00 mm, TR/TE = 3500/10.82 ms, ETL = 8, NSA = 1, bandwidth = 3.7 kHz.

Data analysis

All MRI data analyses were performed by using Matlab (v.7.14; MathWorks, Inc., Natick, USA)

For CEST MRI, data were processed based on the Eqs. 1−2 as described above. For T1rho data a mono−exponential curve fitting was used. That is,

$$\mathrm{SI} = SI_0\, e^{-TSL/T1rho} \qquad [3]$$

where SI and SI_0 refer to the final and initial signal intensities, respectively, TSL is spin locking time, and T1rho is the relaxation time constant in the rotating frame that is to be determined.

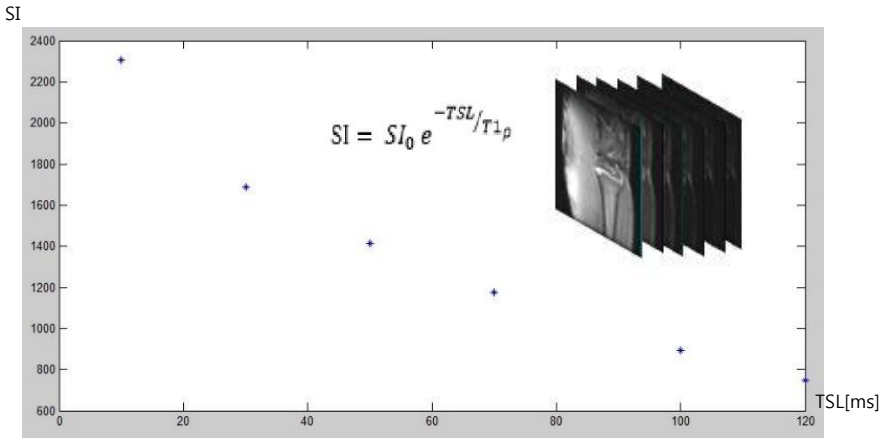

Figure 3 : An overview of how a T1rho relaxation map is made.

All statistical analyses were performed also by using MATLAB.

RESULTS

Representative T1-weighted and T2-weighted MR images are shown in Fig. 4.

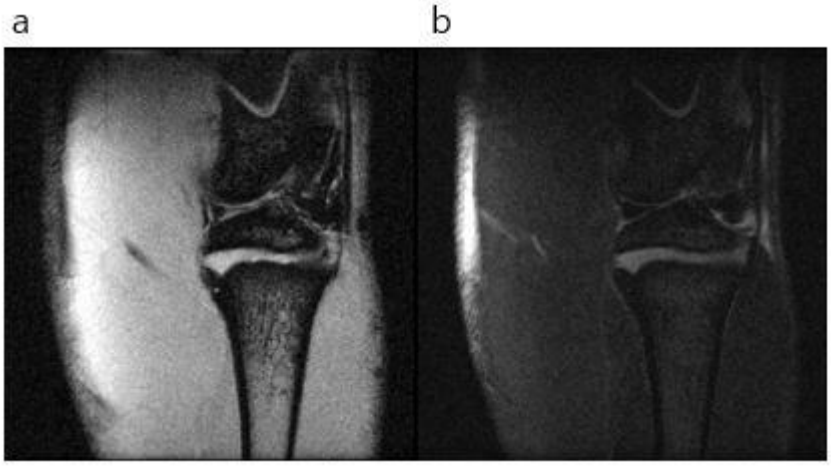

Figure 4 : T1-weighted (a), T2-weighted (b) coronal images of a rat knee joint.

CEST

Figure 5 shows CEST MR images acquired ex-vivo from a swine patella sample at $\delta = \pm 1.0$ ppm.

Figure 6 shows a z-spectrum acquired from the swine patella phantom where S_{sat} and S_0 stand for the signal acquired with and without saturation pulse, respectively. The asymmetry indicates that there are potential target spectral regions for MM quantification using CEST.

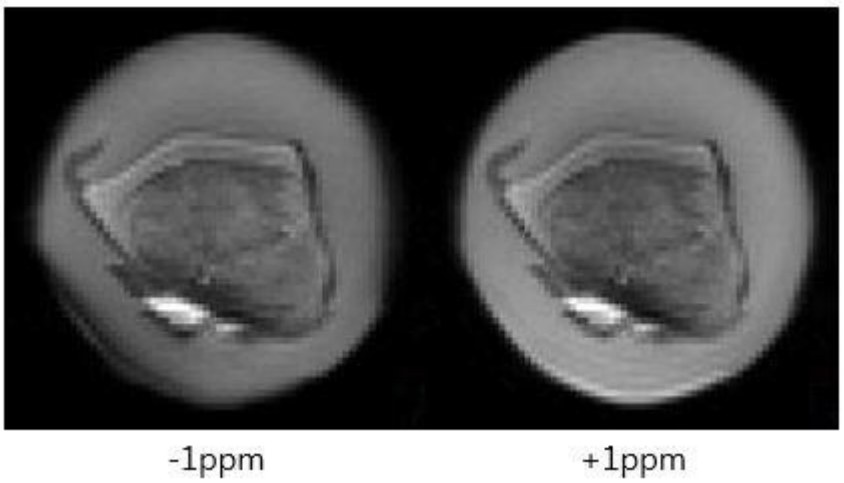

Figure 5 : gagCEST image of swine patella phantom at ±1ppm frequency.

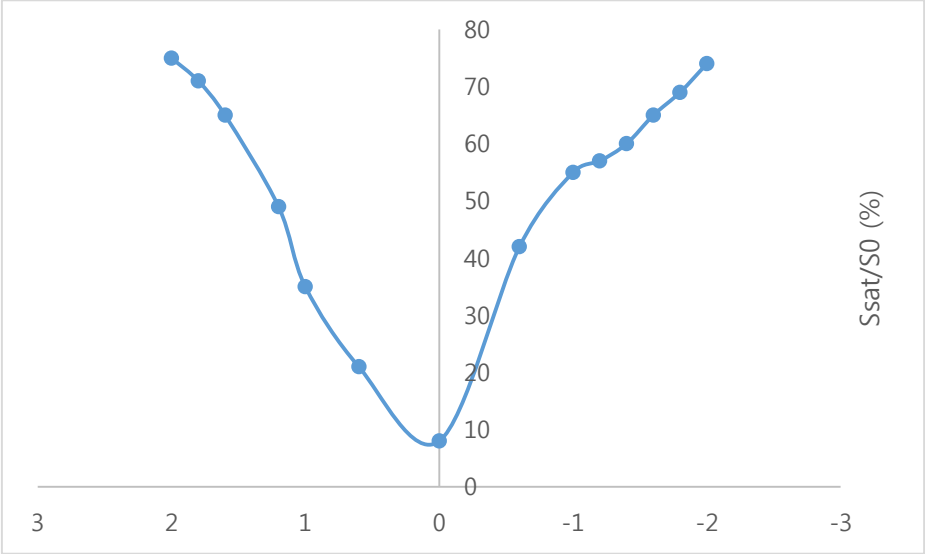

Figure 6 : A CEST z-spectrum with the ROI defined in the swine patella

Figure 7 shows the MTR_{asym} curve from 0.25 ppm to 2.0 ppm. The high asymmetry observed at 1.0 ppm may reflect the

concentrations of the GAG protons groups in cartilage, and therefore used as our target spectral saturation region.

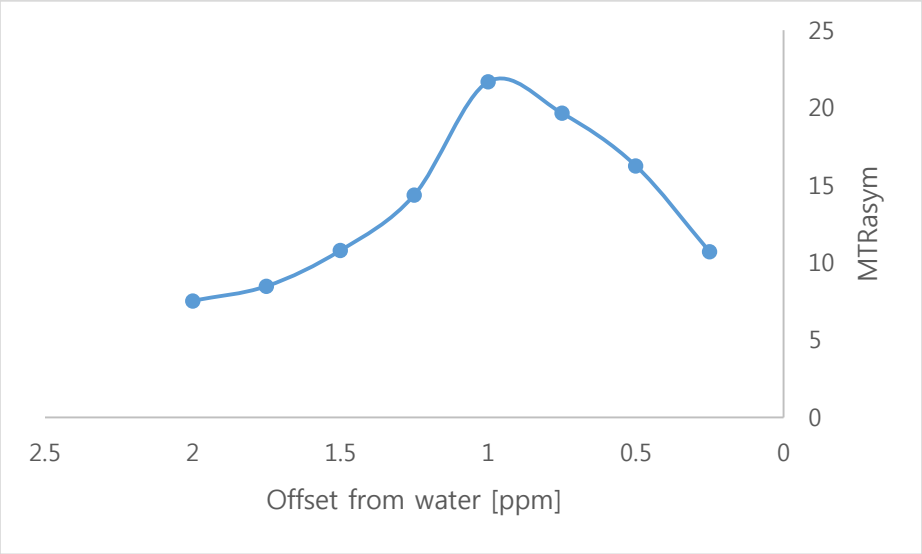

Figure 7 : The MTR asymmetry value is calculated to distinguish the CEST effect.

Figure 8 shows gagCEST MR images acquired in vivo from a rat knee joint. Note that in the difference image, the cartilage region is bright, which demonstrate the potential capability of this MRI technique in monitoring cartilage status. Figure 9 shows gagCEST MTR_{asym} map, where the cartilage contrast is clearly shown..

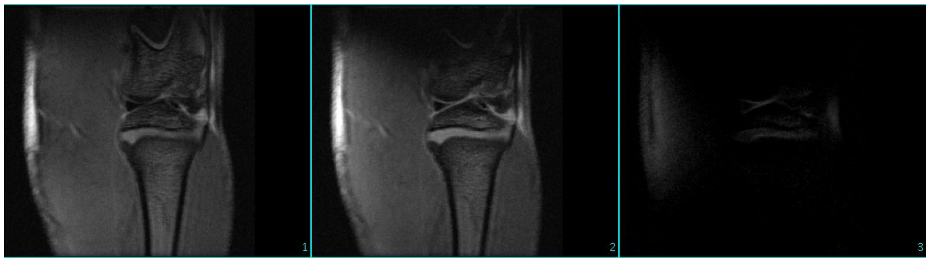

Figure 8 : Images of a rat knee *in vivo* with irradiation at δ = −1.0 ppm, δ = + 1.0 ppm, and the difference image.

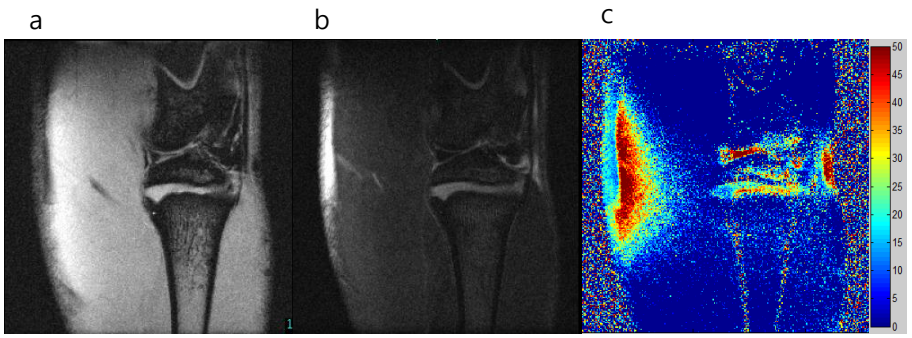

Figure 9 : T1 weighted image (a), T2 weighted image (b), gagCEST map image (c) of a normal rat knee *in vivo*.

Figure 10 shows the distribution of the MTR_{asym} of the cartilages from a total of 16 rats. The 43.77 ± 9.88 of MTR_{asym} values was obtained.

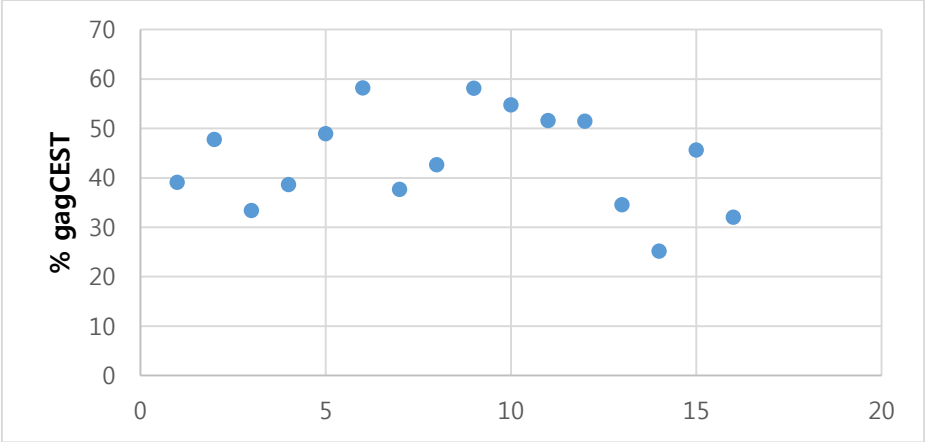

Figure 10 : The MTRasym values from the cartilages of normal male Wistar rats (n=16).

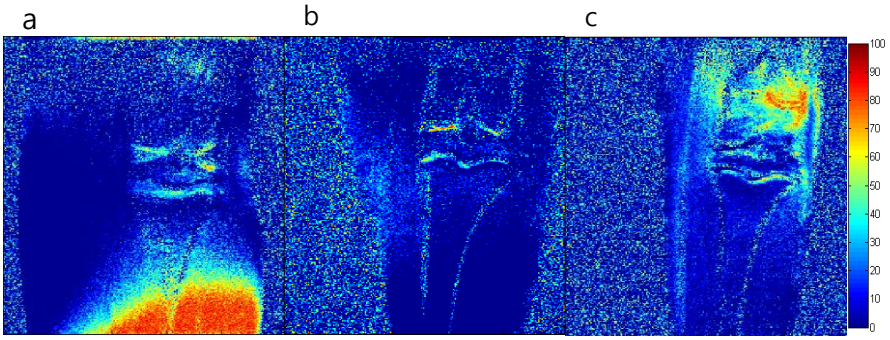

Figure 11 shows gagCEST color map of normal (a), RA (b) and treated (c).

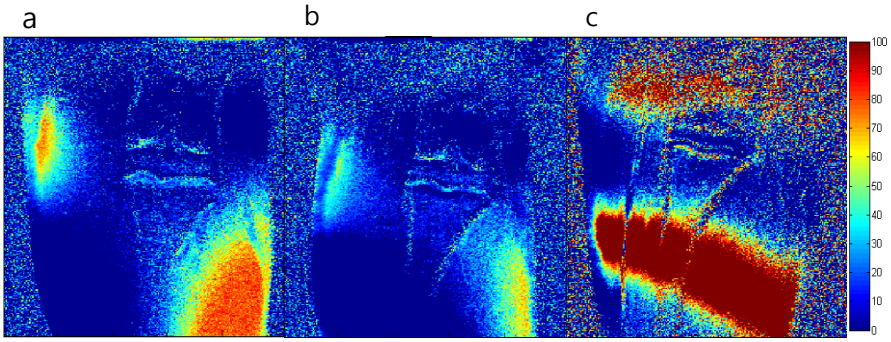

Figure 12 shows gagCEST color map of normal (a), RA model (b) and control (c).

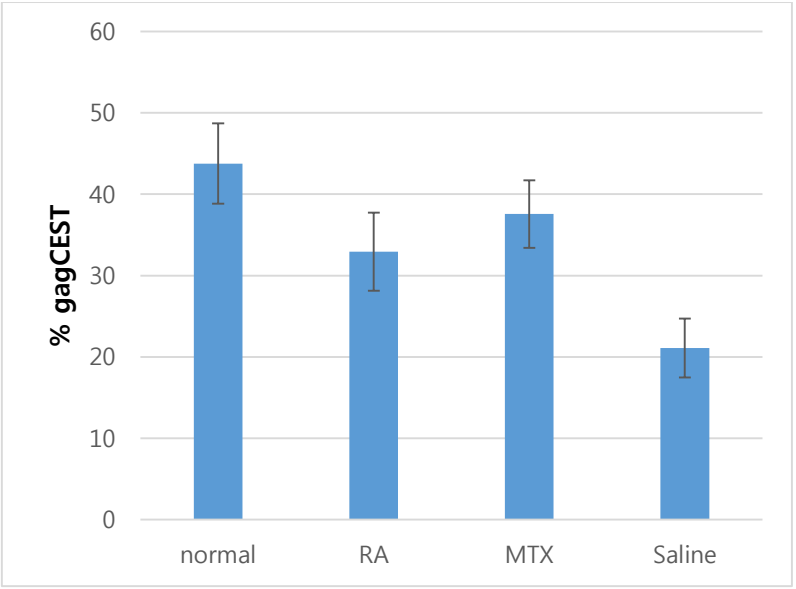

Figure 13 shows percent graph of gagCEST each group.

Figure 11 and figure 12 show gagCEST map of each group (normal, RA, treated, control). RA, treated, and control group could find cartilage loss symptom relative to normal group(43.77 ± 9.88). Percent gagCEST values of treated group were measured 37.57 ± 8.31. Those increase about 14% from RA group(32.92 ± 9.6). However, control group developed rheumatoid arthritis(21.1 ± 7.25) (in Figure 13).

T1rho

Figure 14 shows the T1rho images acquired at TSLs of 10, 20, 30, 40, 50, 70, 100 ms. From these images a T1rho map was

estimated as shown in the figure. For this swine patella phantom, an average of cartilage T1rho value of 56.0 ms was obtained.

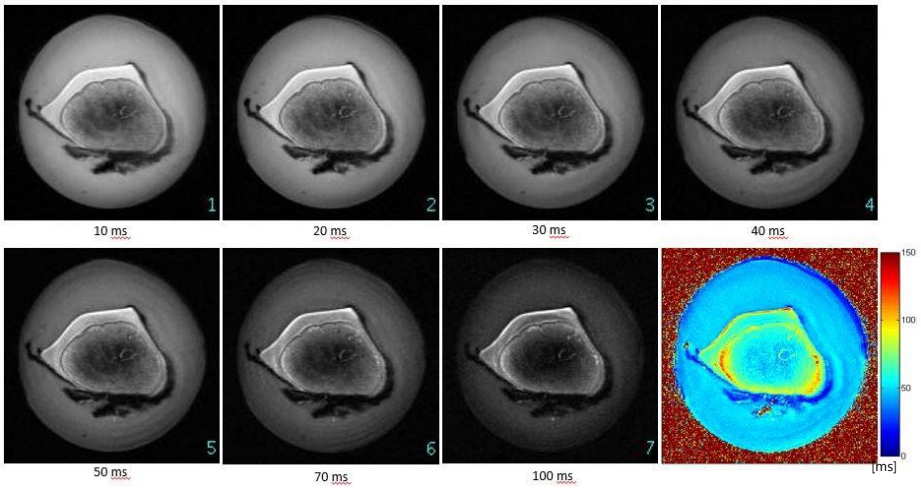

Figure 14 : T1rho images of swine patella phantom at different spin-lock time (TSL=10,20,30,40,50,70,100ms). And T1rho color mapping image.

Figure 15(b) shows T1rho images with TSLs of 10, 30, 50, 70, 100, 120 ms. The exponential signal decay is clearly shown. The corresponding T1rho map is also shown in Fig. 16.

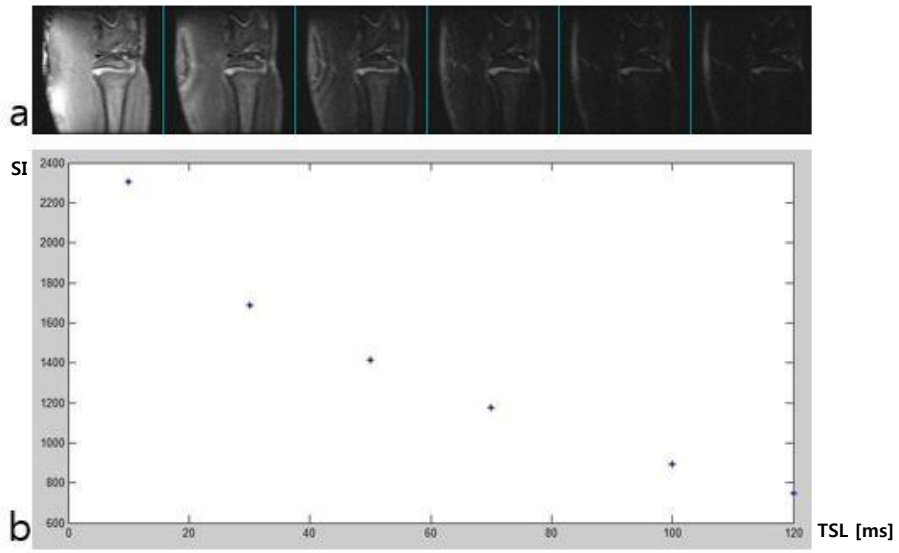

Figure 15 : T1rho images *in-vivo* spin-lock time spacing (a) and T1rho exponential decay plot (b).

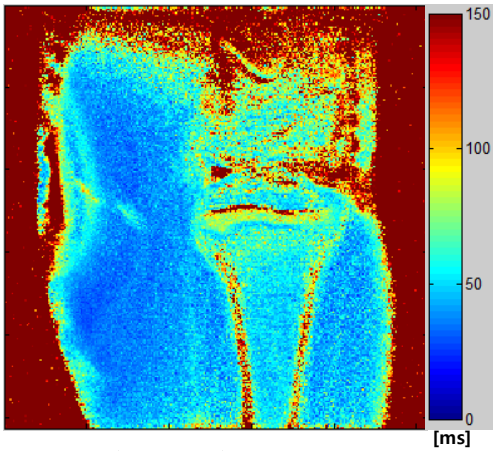

Figure 16 : T1rho color map image *in-vivo* by using mono curve exponential fitting.

Figure 17 shows the distribution of the T1rho values acquired from the cartilages of male wistar rats (n=16). The 82.29 ± 10.05 ms of T1rho value was obtained.

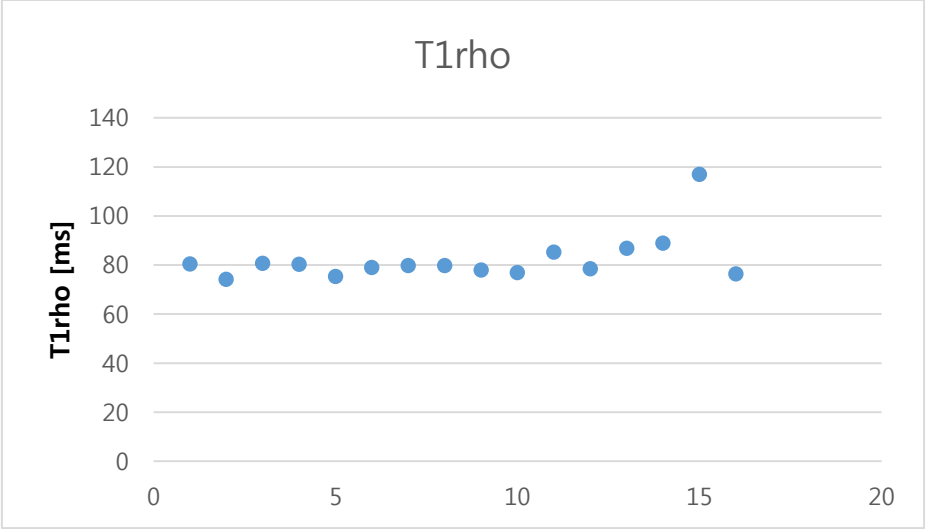

Figure 17 : The T1rho value from normal male wistar rat *in vivo* (n=16).

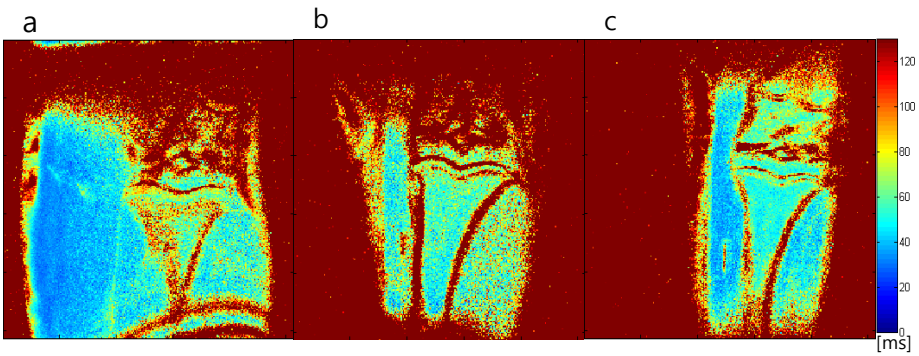

Figure 18 shows T1rho color map of normal (a), RA (b) and treated (c).

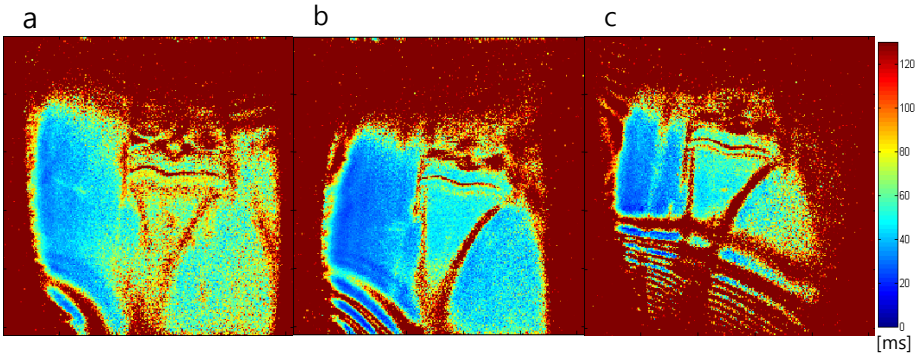

Figure 19 shows T1rho color map of normal (a), RA (b) and control (c).

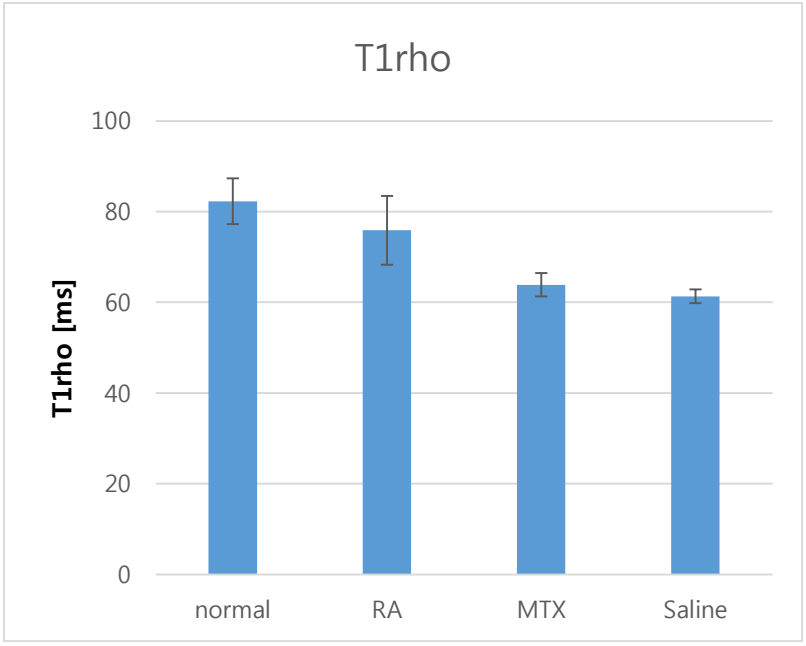

Figure 20 shows graph of T1rho mean value each group.

Figure 18 and figure 19 show T1rho map of each normal, RA, treated, control groups. However, T1rho method cannot validate gag concentration of cartilage (in Figure 20).

DISCUSSION

The GAG concentrations in the cartilage can play an important role in the diagnosis of OA[5]. The dGEMRIC (delayed gadolinium-enhanced MRI of cartilage), which is the current gold standard for cartilage assessment[30], requires contrast agent injection and patient exercise to help the contrast agent diffuse into articular cartilage, thereby resulting in a significantly long procedure time (2~3 hours). gagCEST imaging has been shown to be able to provide information on the molecular composition of cartilage and to identify the early OA change characteristics, such as the loss of GAG content without the need of contrast agent [31]. Despite these potential advantages of gagCEST over dGEMRIC, the implementation of the former at high field can be very challenging as it is highly sensitive to both B_0 and B_1 magnetic field inhomogeneity. For instance, the B_0 inhomogeneity resulting in local resonance frequency shift needs to be addressed in the data analysis. Nonetheless, our preliminary data support that the MRI technique has been successfully implemented on a 9.4T MR scanner. It should be noted that at this high field the improved spectral dispersion would allow for more effective, selective

saturation of the target resonance with reduced direct saturation effect. That is, a better discrimination of the GAG hydroxyl protons from free water protons in CEST spectrum can be brought about at 9.4T.

Our preliminary data also support that the T1rho MRI technique is successfully implemented at high field, which is also prone to B_0 and B_1 field inhomogeneity. A recent study [26] found that cadaveric patella tissue samples with decreased GAG content had increased T1rho relaxation time, despite these same tissues still being within the "normal" T2 relaxation range. Therefore, T1rho may be a more GAG-sensitive measure than T2.

Further studies with more numbers of animals and different animal models of cartilage degeneration are required to compare the performance of the gagCEST and the T1rho methods. However, our preliminary data suggest that the former may be more sensitive to cartilage degeneration than the latter. In this study, we have assumed that T1rho is determined mainly by the amount of MMs whose range of frequencies of molecular motion is close to the Larmor frequency of the spin-locking RF pulse [11]. However, many

other factors can also influence T1rho such as hydroxyl proton exchange, collagen fiber orientation, and other unidentified macromolecules[25]. The limitation of the gagCEST should also be noted. According to recent studies, pH in diseased cartilage may be decreased [30]. This would decrease the MTR measured by gagCEST, thereby resulting in an overestimation of the GAG loss from cartilage [30]. Therefore, in order to further improve the performance of these methods, future work should consider the variable fiber orientation with respect to the external magnetic field and changes in pH in the cartilage, which may be addressed by incorporating diffusion tensor imaging (DTI) and 31P-magnetic resonance spectroscopy (MRS), respectively, into the imaging protocol.

Finally, several technical limitations should be considered for clinical applications of these methods. In this study, T1rho MRI was implemented in combination with a fast spin-echo (FSE) pulse sequence, which is subject to relatively high specific absorption rate (SAR). In the similar context, there is also potential tissue heating issue with these techniques that results from the RF energy during the irradiation of the spin locking RF pulse in T1rho MRI and frequency-selective saturation RF

pulse in gagCEST MRI. These issues can potentially be addressed by alternative designs of the RF pulses in the preparation period. The replacement of FSE with a gradient echo sequence for data acquisition can also facilitate the reduction of overall RF energy during experiments, but at the expense of SNR. In clinical setting, these issues all need to be addressed in consideration of total scan time as well.

CONCLUSIONS

In this study CEST and T1rho MRI techniques were implemented on a 9.4T high field MR scanner. While the potential efficacy of these MRI techniques in cartilage imaging needs to be further validated in animal models with more numbers of animals, previous pioneering studies support that these MRI techniques may facilitate development of a means of non-invasively assessing cartilage degeneration. Those previously reported alterations in these MRI measures in other diseases such as Parkinson's disease, multiple sclerosis, Alzheimer's disease and tumors [12, 14, 23] further support the potential applications of these MRI techniques. For instance, senile plaques and neurofibrillary tangles that are accompanied in early AD are expected to alter bulk water T1rho relaxation times[32].

REFERENCES

1. Chan, W., et al., *Osteoarthritis of the knee: comparison of radiography, CT, and MR imaging to assess extent and severity.* AJR. American journal of roentgenology, 1991. **157**(4): p. 799-806.
2. Mink, J.H. and A.L. Deutsch, *Occult cartilage and bone injuries of the knee: detection, classification, and assessment with MR imaging.* Radiology, 1989. **170**(3): p. 823-829.
3. Roemer, F., et al., *MRI-detected subchondral bone marrow signal alterations of the knee joint: terminology, imaging appearance, relevance and radiological differential diagnosis.* Osteoarthritis and Cartilage, 2009. **17**(9): p. 1115-1131.
4. Haris, M., et al., *Imaging of glutamate neurotransmitter alterations in Alzheimer's disease.* NMR in biomedicine, 2013. **26**(4): p. 386-391.
5. Ling, W., et al., *Assessment of glycosaminoglycan concentration in vivo by chemical exchange-dependent saturation transfer (gagCEST).* Proceedings of the National Academy of Sciences, 2008. **105**(7): p. 2266-2270.
6. Henkelman, R.M., et al., *Quantitative interpretation of magnetization transfer.* Magnetic resonance in medicine, 1993. **29**(6): p. 759-766.
7. Ward, K. and R. Balaban, *Determination of pH using water protons and chemical exchange dependent saturation transfer (CEST).* Magnetic resonance in medicine, 2000. **44**(5): p. 799-802.
8. Santyr, G.E., R.M. Henkelman, and M.J. Bronskill, *Spin locking for magnetic resonance imaging with application to human breast.* Magnetic resonance in medicine, 1989. **12**(1): p. 25-37.
9. Wheaton, A.J., A. Borthakur, and R. Reddy, *Application of the keyhole technique to T1ρ relaxation mapping.* Journal of Magnetic Resonance Imaging, 2003. **18**(6): p. 745-749.
10. De Graaf, R.A., *In vivo NMR spectroscopy: principles and techniques*. 2008: John Wiley & Sons.
11. Jin, T., et al., *Spin-locking versus chemical exchange saturation transfer MRI for investigating chemical exchange process between water and labile metabolite protons.* Magnetic Resonance in Medicine, 2011. **65**(5): p. 1448-1460.
12. Ramani, A., J.H. Jensen, and J.A. Helpern, *Quantitative MR Imaging in Alzheimer Disease 1.* Radiology, 2006. **241**(1): p. 26-44.
13. Bashir, A., et al., *Nondestructive imaging of human cartilage*

glycosaminoglycan concentration by MRI. Magnetic resonance in medicine, 1999. **41**(5): p. 857-865.
14. Wachsmuth, L., H. Juretschke, and R. Raiss, *Can magnetization transfer magnetic resonance imaging follow proteoglycan depletion in articular cartilage?* Magnetic Resonance Materials in Physics, Biology and Medicine, 1997. **5**(1): p. 71-78.
15. Cobb, J.G., J.H. Kan, and J.C. Gore, *T1ρ mapping of pediatric epiphyseal and articular cartilage in the knee.* Journal of Magnetic Resonance Imaging, 2013. **38**(2): p. 299-305.
16. Zhou, J., et al., *Using the amide proton signals of intracellular proteins and peptides to detect pH effects in MRI.* Nature medicine, 2003. **9**(8): p. 1085-1090.
17. van Zijl, P.C., et al., *MRI detection of glycogen in vivo by using chemical exchange saturation transfer imaging (glycoCEST).* Proceedings of the National Academy of Sciences, 2007. **104**(11): p. 4359-4364.
18. van Zijl, P. and N.N. Yadav, *Chemical exchange saturation transfer (CEST): what is in a name and what isn't?* Magnetic Resonance in Medicine, 2011. **65**(4): p. 927-948.
19. Zhou, J. and P. Zijl, *Chemical exchange saturation transfer imaging and spectroscopy.* Progress in Nuclear Magnetic Resonance Spectroscopy, 2006. **48**(2): p. 109-136.
20. Wolff, S.D. and R.S. Balaban, *Magnetization transfer contrast (MTC) and tissue water proton relaxation in vivo.* Magnetic resonance in medicine, 1989. **10**(1): p. 135-144.
21. Redfield, A.G., *Nuclear magnetic resonance saturation and rotary saturation in solids.* Physical Review, 1955. **98**(6): p. 1787.
22. Knispel, R., R. Thompson, and M. Pintar, *Dispersion of proton spin-lattice relaxation in tissues.* Journal of Magnetic Resonance (1969), 1974. **14**(1): p. 44-51.
23. Regatte, R.R., et al., *3D-T< sub> 1ρ</sub>-relaxation mapping of articular cartilage: In vivo assessment of early degenerative changes in symptomatic osteoarthritic subjects1.* Academic radiology, 2004. **11**(7): p. 741-749.
24. Charagundla, S.R., et al., *Artifacts in< i> T</i>< sub> 1ρ</sub>-weighted imaging: correction with a self-compensating spin-locking pulse.* Journal of Magnetic Resonance, 2003. **162**(1): p. 113-121.
25. Stahl, R., et al., *T1rho, T2 and focal knee cartilage abnormalities in physically active and sedentary healthy subjects versus early OA patients—a 3.0-Tesla MRI study.* European radiology, 2009. **19**(1): p. 132-143.
26. Keenan, K.E., et al., *Prediction of glycosaminoglycan content in human cartilage by age, T1ρ and T2 MRI.* Osteoarthritis and Cartilage, 2011. **19**(2): p. 171-179.

27. Regatte, R.R., et al., *Proton spin-lock ratio imaging for quantitation of glycosaminoglycans in articular cartilage.* Journal of Magnetic Resonance Imaging, 2003. **17**(1): p. 114-121.
28. Wheaton, A.J., et al., *Quantification of cartilage biomechanical and biochemical properties via T1ρ magnetic resonance imaging.* Magnetic resonance in medicine, 2005. **54**(5): p. 1087-1093.
29. Brand, D.D., K.A. Latham, and E.F. Rosloniec, *Collagen-induced arthritis.* Nature protocols, 2007. **2**(5): p. 1269-1275.
30. Gold, G.E., et al., *MRI of articular cartilage in OA: novel pulse sequences and compositional/functional markers.* Osteoarthritis and cartilage, 2006. **14**: p. 76-86.
31. Blumenkrantz, G. and S. Majumdar, *Quantitative magnetic resonance imaging of articular cartilage in osteoarthritis.* Eur Cell Mater, 2007. **13**: p. 76-86.
32. Borthakur, A., et al., *T1< sub> ρ</sub> MRI of Alzheimer's disease.* Neuroimage, 2008. **41**(4): p. 1199-1205.

국문 초록

서론: 관절의 장애를 가지는 관절염은 공공 보건에서 큰 어려움으로 여겨진다. 이런 관절염의 초기 증세로서 관절안의 glycosaminoglycan (GAG) 양이 감소되는 것이 보고되었다. 이런 GAG 와 같은 고분자는 TE 가 매우 짧고 일반적인 MR 영상 기법으로는 발견하기 어렵다. 생체 내에서 GAG 와 같은 고분자 량의 변화를 관찰하기 위하여, T1rho 맵과 gagCEST 는 직접 또는 간접적인 관절 성분 측정 MR 영상 기법이다.

방법: gagCEST 와 T1rho 펄스 시퀀스 실험은 팬텀과 동물 생체 실험으로 실시했다. gagCEST 의 경우 다양한 주파수의 포화 펄스로 CEST "z-spectrum"과 MTR_{asym} 을 계산하였다. T1rho 의 경우는 일반적인 FSE 펄스 시퀀스 앞 부분에 스핀 고정 펄스를 연결하였다. 이 스핀 고정 부분의 시간(TSL : spin lock time)을 10, 30, 50, 70, 100, 120 ms 으로 바꿔서 돼지 관절, 생체 랫 무릎 관절 영상을 얻었다. 이렇게 얻은 영상으로 T1rho 맵 영상을 구했다.

결과: gagCEST 의 경우 돼지 관절 팬텀과 생체 랫 무릎 관절 모두 MTRasym = 1.0 ppm 일 경우 가장 높은 값을 나타냈다. gagCEST 의 정량화는 이 CEST 스펙트럼이 1.0 ppm 일 때를 기반으로 한다. 그리고 T1rho 영상의 경우 일반적인 T1 강조영상, T2 강조영상보다 관절 부위

의 신호 대 잡음비 (SNR : signal to noise ratio)가 더 높고, T1rho 맵 영상을 통해서 고분자의 정량화를 분명히 보여준다.

결론: gagCEST 와 T1rho 펄스 시퀀스는 일반적은 MRI 영상 기법으로는 분석하기 어려운 생체 내 고분자를 영상화 하기 위해 만들어진 방법이다. 본 연구를 통해서, 돼지 관절 팬텀과 랫의 생체 내 무릎 관절을 CEST 와 T1rho 영상 기법을 이용하여 실험을 수행했다. 그리고 실험 결과를 통하여, 고자장 (9.4T) MRI 에서 gagCEST 와 T1rho 기법을 이용하여 의미 있는 관절 영상을 얻었다. 추후 알츠하이머병, 암과 같은 다른 고분자 영역 질병에도 적용할 수 있는 가능성을 확인했다.

주요어 : 자기공명영상, 고분자, 정량화, cest, t1rho

학 번 : 2012-23656